

# Crystal engineering of energetic materials: Co-crystals of CL-20



**Post-print of a peer-reviewed article published by the Royal Society of Chemistry.**
**Published article available at: http://dx.doi.org/10.1039/C2CE05796D**

**Cite as:**
**Millar, D. I. A., Maynard-casely, H. E., Allan, D. R., Cumming, A. S., Lennie, A. R., Mackay, A. J., Oswald, I. D. H., Tang, C. C., & Pulham, C. R. (2012). Crystal engineering of energetic materials: Co-crystals of CL-20. *CrystEngComm*, 14(10), 3742-3749.**

**Manuscript received: 25/06/2011; Accepted: 31/01/2012; Article published: 13/03/2012**

# Crystal engineering of energetic materials: Co-crystals of CL-20**

David I.A. Millar,[1,*] Helen E. Maynard-Casely,[1] David R. Allan,[2] Adam S. Cumming,[3] Alistair R. Lennie,[2] Alexandra L. Mackay,[1] Iain D.H. Oswald,[1,4] Chiu C. Tang[2] and Colin R. Pulham[1]

[1]EaStCHEM, School of Chemistry and Centre for Science at Extreme Conditions, Joseph Black Building, University of Edinburgh, West Mains Road, Edinburgh, EH9 3JJ, UK.

[2]Diamond Light Source Ltd, Harwell Science and Innovation Campus, UK.

[3]Defence Science and Technology Laboratory, Fort Halstead, Sevenoaks, UK.

[4]Strathclyde Institute of Pharmacy and Biomedical Sciences, University of Strathclyde, 27 Taylor Street, Glasgow, UK.

[*]Corresponding author; e-mail: D.I.A.Millar@sms.ed.ac.uk, fax: +44 (0) 131 650 4756, tel: +44 (0) 131 650 6752

[**]We thank Dstl and EPSRC for contributions toward a studentship (DIAM), and MOD WPE for funding under the terms of contract RD028-06366. Part of this work was carried out with the support of Diamond Light Source. We would also like to acknowledge F. White and N. Funnell (UoE) for the collection of single-crystal diffraction data and J.W. Fang for the translation of Chinese manuscripts.[25, 29, 30]

**Supporting information:**
[†] Electronic supplementary information (ESI) available: Crystallographic information files and Raman spectra for all of the structures are included. In addition, we have supplied a short video of the reaction between CL-20 and piperidine, as well as a photo of the residue (currently being characterised). Caution: Energetic materials present a significant safety hazard due to their inherent explosion risk upon initiation by impact, shock, heat or friction. Crystallisation studies should therefore be conducted on a very small scale (as detailed below) using non-spark apparatus, Kevlar personal protection and a blast screen. This is especially true of co-crystallisation experiments, since the sensitivity and thermal stability of new co-crystals is unknown. To illustrate the potential for violent exothermic reactions of CL-20, we have supplemented this article with a video of the vigorous reaction of CL-20 with piperidine. CCDC reference numbers 832144–832147. For ESI and crystallographic data in CIF or other electronic format see http://dx.doi.org/10.1039/C2CE05796D

**Abstract**

Co-crystallisation is proposed as an effective method to adapt the physico-chemical properties of energetic materials, thus presenting the opportunity to fine-tune performance characteristics at the molecular level. This is illustrated by the characterisation of four co-crystals of the high explosive CL-20.

**Main text**

Energetic materials represent an important class of compounds that contain large amounts of stored chemical energy within their molecular structures and which can undergo rapid decomposition to produce large quantities of hot gaseous products. These high-energy-density materials (encompassing propellants, explosives and pyrotechnics) have applications that include mining, armaments, space exploration and fireworks. For many applications, reproducible and reliable performance is essential especially when these materials may be exposed to a range of environments, *e.g*. long-term storage, elevated temperatures, impact from shrapnel, mechanical shock and friction. Properties that are critical to energetic performance include sensitivity to detonation (by impact, friction, shock or charge); the detonation velocity; thermal stability and crystal morphology. As a result of these stringent performance criteria, current energetic formulations are based on a very small number of compounds. An increasingly important consideration for energetic materials is their sensitivity to accidental initiation and this is leading to the development of "insensitive munitions".[1]

Current strategies for reducing sensitivity involve the embedding of crystallites of the explosive or propellant in a polymer binder. The binder serves the purpose of dissipating the energy of impact/friction and reduces the likelihood of initiation *via* hot-spots. Another strategy is the use of reduced sensitivity components in the polymer-bonded explosive (PBX). Several companies now market so-called "reduced-sensitivity (RS) RDX" that is claimed to exhibit reduced sensitivity to accidental initiation and which hence commands a premium for certain applications. The details of such formulations are proprietary information and so despite a number of investigations by laboratories around the world, it is not yet clear what is responsible for the reduced sensitivity. Factors such as purity, particle size, particle morphology, number of voids, and number of defects have all been suggested to play a role.[2] Another strategy that has been deployed is the development of new energetic materials that are intrinsically less sensitive. Recent examples include FOX-7 (1,1-diamino,2,2-dinitroethene) and FOX-12 (guanylurea dinitramide). It has been suggested that the reason for the intrinsic insensitivity of these materials lies in the way that these molecules pack together in the crystals. Both compounds adopt structures in which the molecules are arranged in layers linked by relatively strong hydrogen bonds – it is believed that such structures allow energy to be dissipated efficiently throughout the crystal thereby reducing the likelihood of initiation *via* hot-spots.[3] A novel and intriguing approach that has very recently been suggested is the use of co-crystallisation to enhance the energetic performance of existing materials and as a possible method of improving the viability of other candidate materials.[4, 5]

It is well documented that co-crystallisation is an effective technique for the modification of the physico-chemical propertes of crystalline solids.[6-8] Such attempts at crystal engineering are nowhere more evident than in the pharmaceutical sector, where it may be desirable to improve factors such as dissolution rate, thermal stability and bioavailability without the structural adaptation of the active pharmaceutical ingredient (API).[9, 10] In contrast to typical APIs, which generally have a range of functional groups that can be exploited for crystal engineering, typical energetic molecules have a much narrower range of functionality (often restricted to nitro-groups). This is perhaps reflected in the scarcity of structural data reported for co-crystals of energetic materials. Although numerous solvates of the high explosives HMX (1,3,5,7-tetranitro-1,3,5,7-tetraazacyclooctane) and RDX (1,3,5-trinitrohexahydro-1,3,5-triazine) have been identified spectroscopically,[11, 12] only six of these have been structurally characterised.[13-16] In addition, 2,4,6-trinitrotoluene (TNT) has recently been the subject of a thorough co-crystallisation screening, the result of which was the structural characterisation of 17 co-crystals of TNT with a range of aromatic and heterocyclic co-formers.[4] Therefore, in order to exploit the potential for new energetic co-crystals with tailored properties, it is necessary to develop a library of supramolecular synthons suitable for their rational design.

In this work we have studied the co-crystallisation of the polycyclic nitramine 2,4,6,8,10,12-hexanitrohexaazaisowurtzitane (HNIW), commonly referred to CL-20 on account of its development at China Lake, USA.[17] CL-20 (shown in Figure 1) is currently the most powerful explosive available commercially, although concerns remain over its sensitivity to detonation.[18] It would therefore be desirable to obtain CL-20 in a form that displays sufficiently reduced sensitivity, without compromising explosive performance. Recent studies have focussed on the development of CL-20-based PBXs.[19-21]

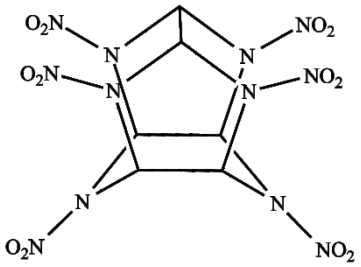


***Figure 1.*** Molecular structure of CL-20

In order to provide an alternative route to insensitive CL-20-based munitions, we have conducted co-crystallisation trials with a range of organic co-formers. The conformational flexibility displayed by the CL-20 molecule, a feature it has in common with HMX, may lead one to expect this material to be an ideal candidate for such an approach. The structure consists of a rigid isowurtzitane cage with nitro groups attached to each of the bridging nitrogens. The relative orientations of these nitro groups to the isowurtzitane cage, together with

the crystal packing, gives rise to the rich polymorphism that has been explored in detail in previous studies.[17, 22, 23] Of the 24 possible conformers, DFT calculations on the *isolated* molecule have shown that the four most stable arrangements correspond to those observed experimentally in the crystalline state, reflecting the relatively small energy barriers that exist between these conformations, see Figure 2.[24]

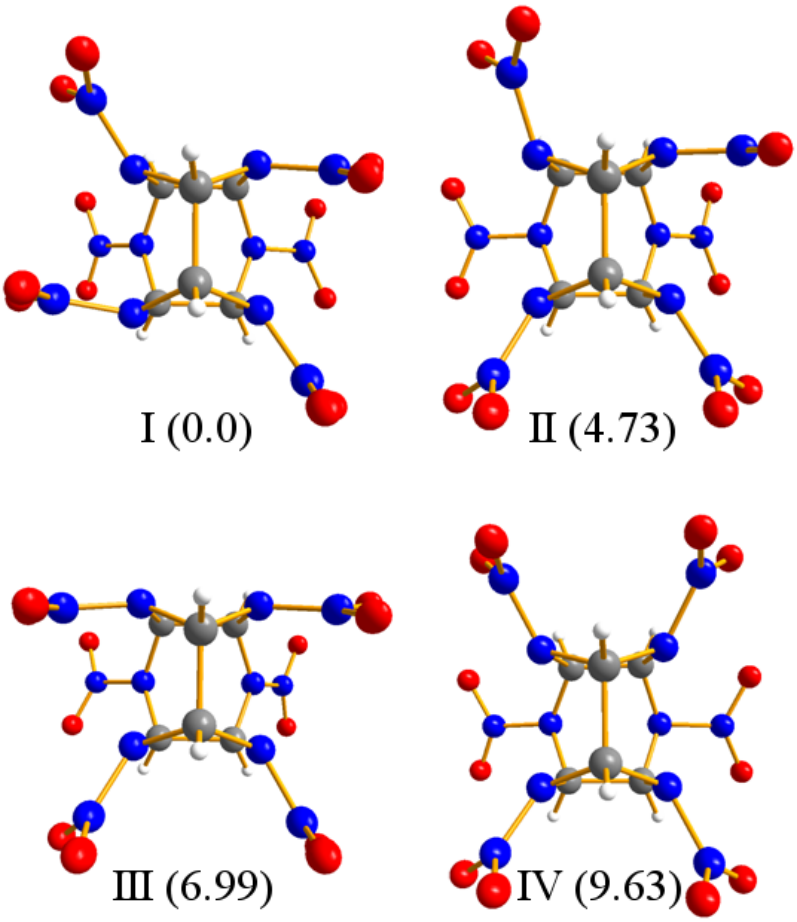


***Figure 2.*** The most stable molecular conformations and the polymorph in which they are observed (the relative energies, in kJ mol$^{-1}$, calculated by Kholod *et al*.[24] are also shown). The conformation shown in I is adopted by β-CL-20, II is exhibited in both the α- and γ-forms, while ε-CL-20 adopts conformation III.[17] The high-pressure form, ζ-CL-20, adopts conformation IV.[23]

We therefore present the full structural refinements for four binary co-crystals of CL-20, with *N*,*N*-dimethylformamide (DMF), 1,4-dioxane, hexamethylphosphoramide (HMPA) and γ-butyrolactone. It should be noted that the DMF adduct of CL-20 has been reported previously but no detailed discussion of the structure was presented.[25]

**Results**

A summary of the structural information for each of these co-crystals can be found in Table 1.

***Table 1.*** Crystallographic information for the four co-crystals of CL-20

| | **DMF** | **1,4-dioxane** | **HMPA** | **butyrolactone** |
|---|---|---|---|---|
| S.G. | *P*-1 | *P*-1 | $P2_1/c$ | *Cc* |
| *a* (Å) | 7.7843(16) | 10.3061(3) | 18.8930(3) | 15.7503(9) |
| *b* (Å) | 12.857(3) | 10.7691(3) | 12.07295(13) | 20.5096(13) |
| *c* (Å) | 13.002(3) | 14.5298(4) | 21.8241(4) | 23.2073(13) |
| *α* (°) | 113.73(2) | 73.897(2) | 90 | 90 |
| *β* (°) | 106.34(3) | 89.527(2) | 114.977(2) | 90.092(2) |
| *γ* (°) | 92.43(3) | 85.057(2) | 90 | 90 |
| *V* (Å$^3$) | 1125.1(6) | 1543.38(8) | 4512.41(14) | 7496.7(8) |
| $D_c$* (Mg m$^{-3}$) | 1.725 | 1.606 | 1.436 | 1.856 |
| *T* (K) | 150 | 150 | 100 | 100 |
| Stoichiometry | 1:2 | 1:4 | 1:3 | 1:1 |
| CL-20 conformation | γ | γ | β | γ |

*For reference, the crystal density of ε-CL-20 is 2.083 Mg m$^{-3}$ at 100 K.[26]

**CL-20:DMF** (in a 1:2 ratio) has been found to crystallise in the triclinic crystal system ($P\bar{1}$), in which the molecules are broadly arranged in alternate layers of CL-20 and DMF, as shown in Figure 3(a). In the DMF layer, both independent molecules each form dimers over inversion centres oriented such that the carbonyl group of each molecule is directed along the interplanar direction. The result of this is that no significant intermolecular interactions occcur between the DMF molecules – the closest contacts exist between the hydrogen atoms of the methyl groups (at 2.323(1) and 2.983(1) Å, respectively). Similar contacts exist between the dimers themselves, resulting in a planar arrangement of the co-former molecules.

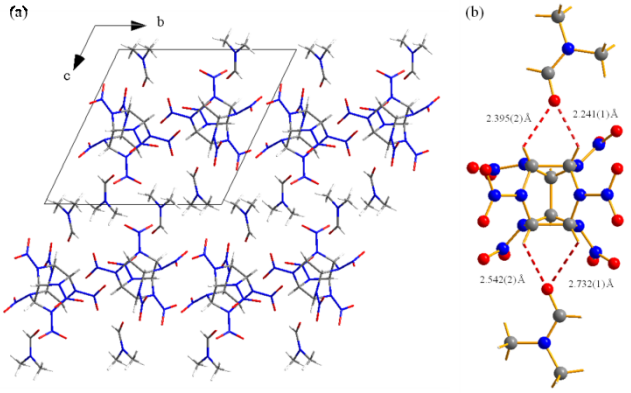


***Figure 3.*** (a) the layered arrangement observed in CL-20:DMF (viewed down the *a*-axis; (b) the intermolecular C-H…O interactions between the layers of CL-20 and DMF molecules.

Within the CL-20 layers, the individual molecules adopt both the molecular conformation and the relative spatial distribution observed in the γ-polymorph of the unsolvated material. The 'face-to-face' arrangement (whereby all five-membered rings of the cage are oriented about the same axis) results in a network of weak C-H…O interactions linking CL-20 molecules along two dimensions. In the third direction, perpendicular to the layers, the most significant intermolecular interaction occurs between the oxygen atoms of the DMF molecules and the C-H groups along two of the cage edges (see Figure 3(b)), ranging from 2.241(1) to 2.732(1) Å.

The contacts between CL-20 and dioxane molecules are limited to weak C-H…O interactions (*ca* 2.7 – 2.8 Å) – this is reflected in the relatively low desolvation temperature. Desolvation was observed by a dramatic difference between the Raman spectra obtained at 313 and 323 K; at the latter temperature the characteristic spectrum for γ-Cl-20 was observed. It is interesting to note that this temperature is *ca* 100 K below the reported ε → γ transition in the non-solvated material.[27]

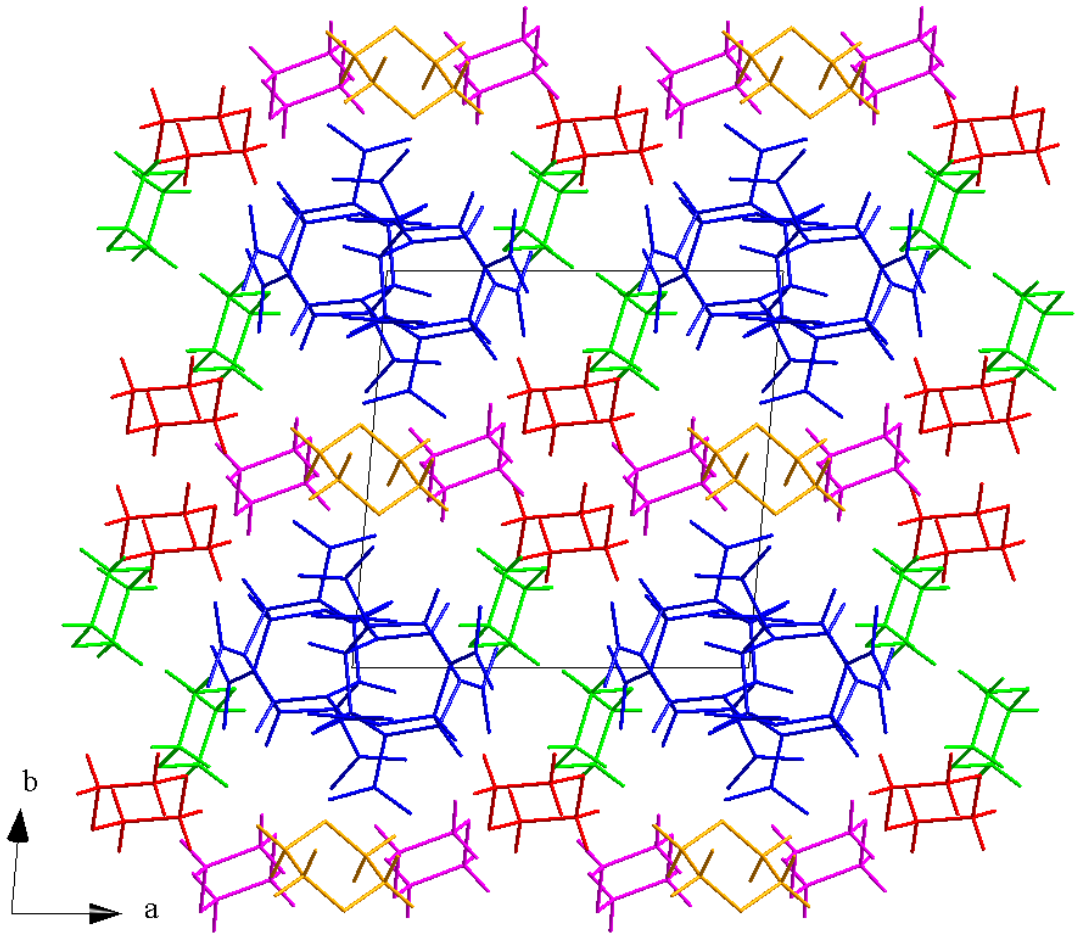


***Figure 4.*** Super cell (2 x 2 x 2) showing the crystal packing in CL-20:dioxane, viewed down the *c*-axis. It should be noted that each colour represents a crystallographically independent molecule; only one orientation of the disordered dioxane molecule (red) is shown for clarity.

In the crystal structure (monoclinic, $P2_1/c$) of **CL-20:HMPA**, two independent molecules of HMPA are positioned such that the phosphorus-oxygen double bond is oriented directly at the hydrogen atoms of opposite faces of the isowurtzitane cage, as shown in Figure 5(a). Meanwhile, a third HMPA molecule completes a shell of co-former molecules that surrounds a 'dimer' of CL-20 molecules situated over an inversion centre (see Figure 5(b)).

Excluding the C-H…O interactions between the molecules of the dimer, which, at 2.430(2) Å, are shorter than similar contacts observed in any of the pure polymorphs, there are no significant CL-20…CL-20 intermolecular interactions in this structure. It may therefore be regarded as a lattice composed solely of HMPA molecules; voids in this lattice are then filled by the CL-20 dimers. Finally, the layered nature of the overall structure also becomes evident when viewed down the monoclinic axis (Figure 5(b)). The molecules are arranged in zig-zag chains along the face diagonal with remarkably few inter-chain interactions.

Desolvation of CL-20:HMPA results in the formation of β-CL-20, the polymorph with which it shares its molecular conformation. In contrast to CL-20:dioxane, however, desolvation does not occur until *ca* 413 K, as determined by variable temperature Raman spectroscopy. This relatively high desolvation temperature is perhaps indicative of the strength of the intermolecular interactions that occur between the CL-20 and HMPA molecules.

The crystal structure of **CL-20:γ-butyrolactone** was initially determined by X-ray powder diffraction. Indexing of the high-resolution powder diffraction pattern suggested an orthorhombic unit cell [$Pna2_1$; $a$ = 23.2762, $b$ = 10.2938, $c$ = 7.8935 Å], with which it was possible to perform structure solution by global optimisation methods (using the program FOX).[28] However, upon re-inspection of the Rietveld refinement of the diffraction pattern it became clear that the proposed orthorhombic structure did not accurately model the very weak diffraction intensities, for example those observed at 5.6 and 9.0° (see Figure 6). Despite further indexing trials that included the peaks highlighted in Figure 6, it was not possible to obtain a definitive unit cell based on the powder diffraction data. Our efforts therefore became focussed on obtaining a single crystal suitable for single-crystal X-ray diffraction. Subsequently, structure solution based on single-crystal data showed that CL-20:butyrolactone (in a 1:1 ratio) in fact adopts a very complicated structure, in which there are four independent CL-20 molecules in the asymmetric unit.

Comparison of the monoclinic structure ($Cc$) determined by single-crystal diffraction with the initial orthorhombic structure, depicted in Figure 7, highlights a number of similarities between the solutions. Firstly, both structures exhibit the CL-20 molecule in the γ-conformation, despite the ε-conformation being input into the global optimisation software. Secondly, the distribution of the CL-20 and butyrolactone molecules is broadly consistent between the two solutions. Thirdly, initial inspection of the two unit cells may suggest they be related, *i.e*. the $b$- and $c$-parameters of the orthorhombic indexing are doubled to produce the monoclinic unit cell and the monoclinic $\beta$-angle remains close to 90°. However, no sub-group relationship exists between the space groups $Pna2_1$ and $Cc$. Furthermore, close examination of each of the solutions shows that the

reduction in symmetry results in a very subtle change in the crystal packing. While nearest-neighbour intermolecular interactions may be comparable in both solutions, structural overlap becomes considerably worse as we progress away from the origin. Finally, demonstrable proof that the monoclinic solution is, indeed, correct, was obtained by Rietveld refinement of the X-ray powder diffraction pattern obtained using the single-crystal structure as the starting model.

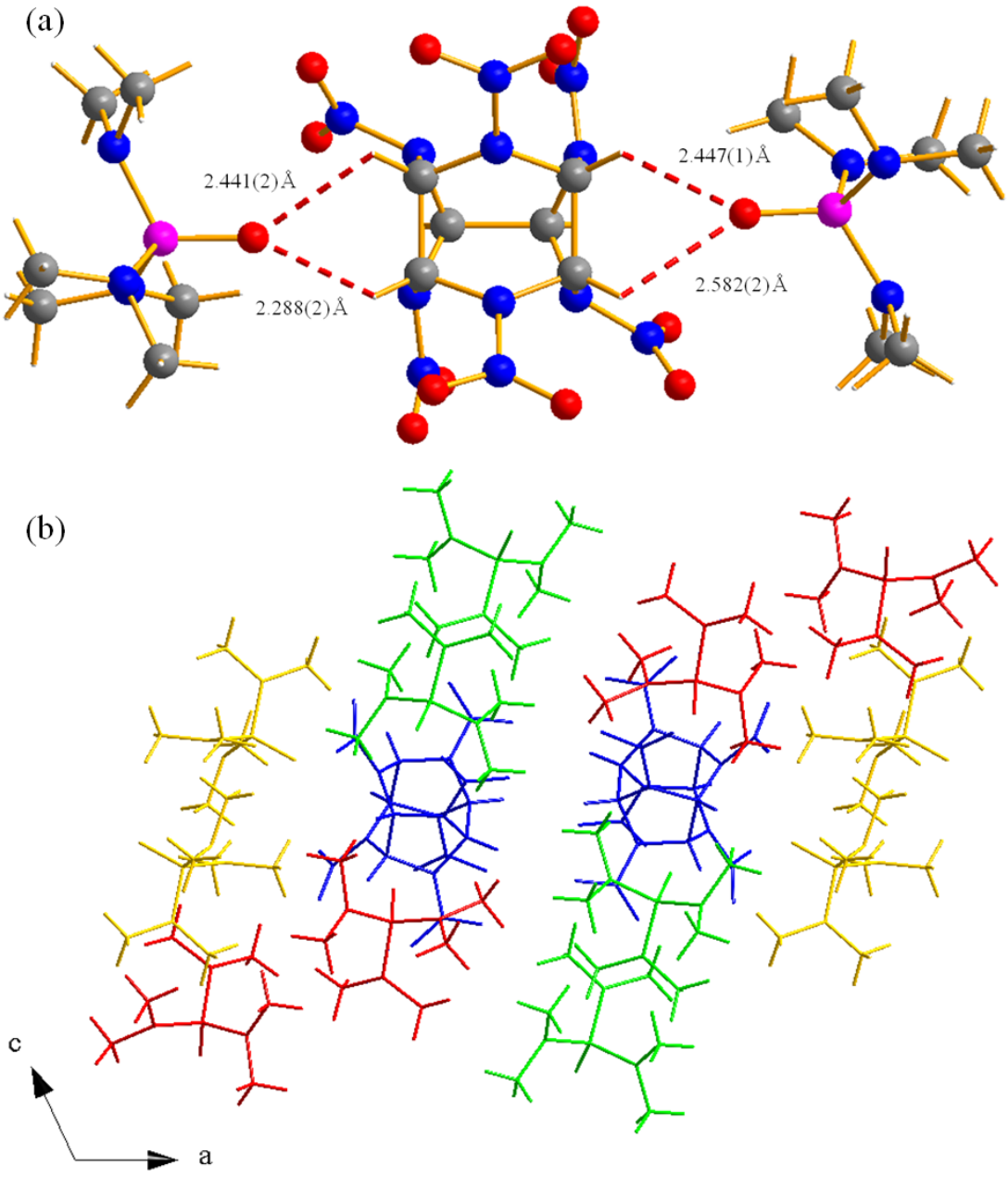


***Figure 5.*** (a) The short intermolecular contacts between two independent HMPA molecules and the CL-20 molecule; and, (b) the CL-20 dimer (blue) surrounded by a shell of HMPA co-formers (coloured by symmetry equivalence). This perspective also demonstrates the layered nature of this structure.

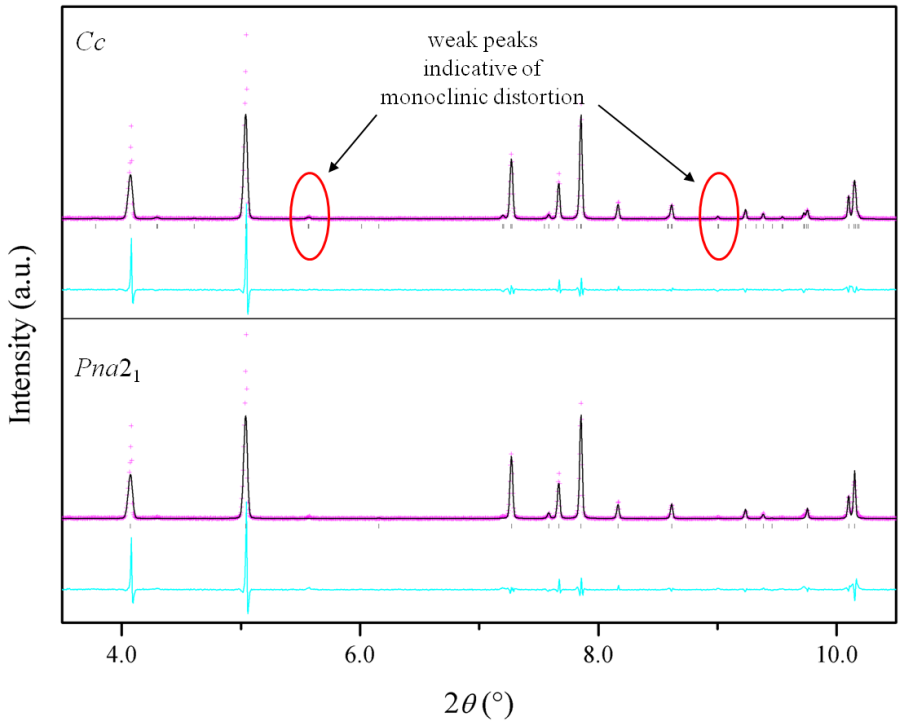


***Figure 6.*** Comparison of the Rietveld refinements of the diffraction pattern collected for CL-20:γ-butyrolactone (150 K) using both the initial $Pna2_1$ solution (bottom) and the *Cc* structural model (top). The experimental data ($I_{obs}$) are shown as pink crosses, the calculated patterns ($I_{calc}$) as a black line and the difference between these models ($I_{obs} - I_{calc}$) is shown in cyan. The weak peaks that are indicative of the true monoclinic nature of this structure are highlighted.

As shown in Figure 8, four independent CL-20 molecules are observed in the asymmetric unit, all of which adopt the γ-conformation with minimal variation between them. When viewed down the *a*-axis, the CL-20 molecules may be considered to be arranged in layers, which themselves may be sub-divided into layer A and B. Layer A contains alternating CL-20 molecules 1 (magenta) and 2 (green), while the same arrangement of molecules 3 (blue) and 4 (red) can be found in layer B. Within both layers A and B, the CL-20 molecules adopt the 'face-to-face' arrangement, giving rise to chains running parallel to the *a*-axis, linked by weak C-H…O interactions (ranging from 2.326(6) to 2.663(6) Å). Similar interactions arise between layers A and B, resulting in a zig-zag network of CL-20 molecules in the *ab*-plane.

A similar distribution of molecules is observed in the γ-butyrolactone layers, which occur between the CL-20 layers (see Figure 8(b)). The co-former molecules may therefore be considered to form two chains running parallel to the *a*-axis, each of which consists of two independent molecules. It is interesting to note that the carbonyl group of every molecule is oriented approximately perpendicular to the direction of the chain. Hence, no signficant intermolecular interactions are observed between γ-butyrolactone molecules themselves. It should also be noted that it has been necessary to refine one of the co-former molecules over two sites (each

with half occupancy), although this disorder changes significantly neither the crystal packing nor the intermolecular interactions.

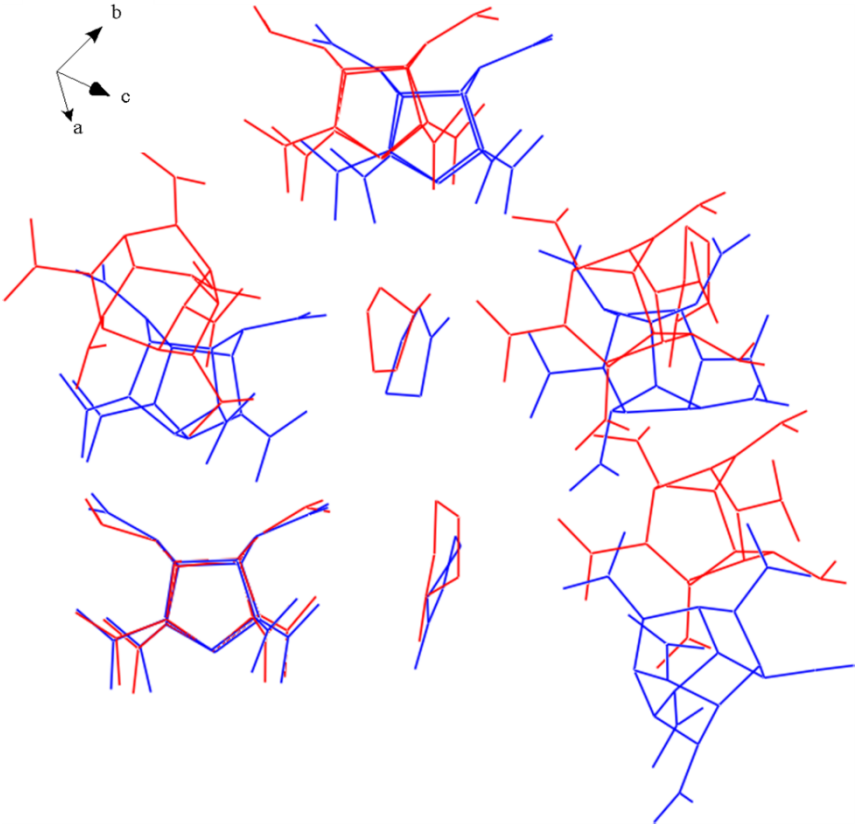


***Figure 7.*** Structure overlay of the *Pna*2$_1$ powder diffraction solution (shown in red) and the *Cc* structure determined in the single-crystal diffraction experiment (blue). The structures have been oriented such that the one CL-20 molecule of the *Pna*2$_1$ structure is superimposed on a corresponding molecule in the *Cc* structure. Hydrogen atoms have been omitted for clarity.

Interplanar interactions are dominated by C-H…O interactions between the hydrogen atoms of the isowurtzitane cages and the oxygen atoms of the co-formers. As shown in Figure 8(c), the butyrolactone molecules are situated such that the ring oxygen interacts with its nearest neighbouring CL-20 molecule (2.287(6) – 2.411(6) Å), while the carbonyl oxygen is in close proximity to the nearest neighbour *and* the next molecule in the CL-20 chain (2.279(7) – 3.073(7) Å). In this way, the CL-20/butyrolactone interactions may be viewed as an extended chain that runs along the *a*-axis.

The thermal stability of CL-20:butyrolactone was also investigated by variable temperature Raman spectroscopy. Desolvation was observed to occur at 376 K, as indicated by the characteristic Raman spectrum of the γ-form of the unsolvated material. This desolvation temperatues lies between that observed for CL-

20:dioxane and CL-20:HMPA, perhaps suggesting a hierarchy of the intermolecular interactions in these co-crystals: CL-20:HMPA > CL-20:γ-butyrolactone > CL-20:dioxane.

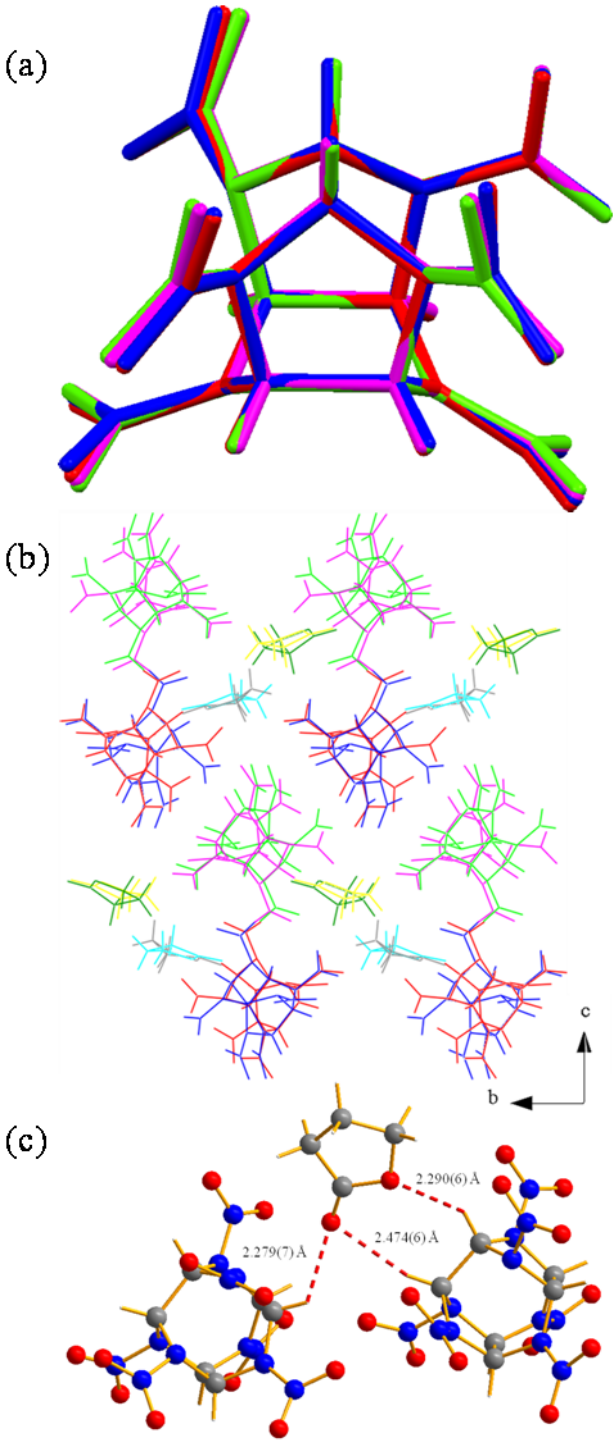


***Figure 8.*** (a) The four independent CL-20 molecules in the asymmetric unit; (b) crystal packing in CL-20:γ-butyrolactone viewed down the *a*-axis, highlighting the layered structure; (c) an example of the CL-20:γ-butyrolactone intermolecular interactions.

**Discussion**

Although this survey of CL-20 co-crystals is by no means exhaustive, comparison of the structures determined for these four cases may provide important information regarding the dominant intermolecular interactions and the favourability of different CL-20 molecular conformations. Thus we have shown that in the absence of traditional crystal engineering motifs (such as hydrogen bonding or π…π stacking), co-crystal formation appears to be directed by much weaker C-H…O and P=O…H intermolecular interactions. This observation is in accordance with IR and NMR spectroscopic studies which have shown that the solvents DMF, dioxane, HMPA, dimethylsulfoxide (DMSO) and γ-butyrolactone are capable of forming molecular complexes with CL-20.[29, 30] This information is extremely valuable since it may allow the rational selection of candidate co-former molecules, thus streamlining future crystallisation trials.

The conformations observed for the CL-20 molecules in the four co-crystals illustrate the delicate balance of intra- and intermolecular interactions in the solid state. Thus, three of the structures display the CL-20 molecule in the γ-conformation and one in the β-conformation. The γ-conformation is also observed in the hemihydrate (α-CL-20)[17] and the $CO_2$-inclusion compound recently reported by Saint Martin *et al.*[31] While it is difficult to draw conclusions based on so few examples, there is perhaps a trend in the co-crystals towards the adoption of molecular conformations that more closely mirror the relative conformational energies of *isolated* CL-20 molecules, namely β: 0.0 kJ $mol^{-1}$; γ: 4.73 kJ $mol^{-1}$; ε: 6.99 kJ $mol^{-1}$; and, ζ: 9.63 kJ $mol^{-1}$.[24] It is also interesting to note that, in the case of CL-20:dioxane, CL-20: HMPA and CL-20:butyrolactone, desolvation results in the γ-form of the unsolvated material, the polymorph with which they share their molecular conformation. Furthermore, in each of these cases the characteristic Raman spectrum of γ-CL-20 was observed at a temperature considerably lower than that at which the ε → γ is observed in pure CL-20. It is clear from this observation that, in addition to altering the energetic performance in the solid state, co-crystallisation may be viewed as a highly-discriminating method for polymorph selection and indeed may provide crystallisation pathways to novel polymorphs.

In terms of the practical application of energetic co-crystals it is important to assess the explosive performance of these materials, particularly with reference to the pure materials. From these results it is immediately clear that the inclusion of co-former molecules leads to a reduction in crystal density, and should therefore result in a decreased detonation velocity.[32] However, Matzger has shown that, at least for some TNT cocrystals, this reduction in density is not observed[4], suggesting that high-density co-crystals of CL-20 may yet be discovered.

Clearly the incorporation of another non-energetic co-former will result in a substantial decrease in explosive power, *i.e*. the energetic component has been diluted. Given the superior explosive power of CL-20 with respect to other common explosives *e.g*. HMX[18] , it may be possible to obtain a CL-20 co-crystal with reduced sensitivity which retains sufficient explosive power. Of course, the loss of explosive power can be overcome by co-crystallisation with compounds which are themselves energetic.

Detailed sensitivity tests on these co-crystals are currently being performed to assess quantitatively changes in sensitivity. Qualitatively, we have not observed any dramatic increases in sensitivity during manipulation. Given the layered motifs observed for three of the structures it is possible that these co- crystals might display improved stability to friction or shock through dissipation of energy through the layers. The remarkable insensitivity to detonation of FOX-7, for example, has been attributed to a similar layered packing in the crystalline state, although FOX-7 also displays significant intermolecular hydrogen bonding.[3]

**Conclusions**

Co-crystallisation is proposed as an attractive route to the modification of the physico-chemical properties of energetic materials, thereby presenting the opportunity to dramatically alter explosive performance. The potential for obtaining energetic co-crystals of the high explosive CL-20 has been demonstrated by the structural analysis of four co-crystals. This was particularly challenging given the absence of traditional supramolecular synthons used in crystal engineering (*e.g*. hydrogen bonding). In addition to the analysis of the intermolecular interactions, it has been shown that the conformational flexibility of the CL-20 molecule is an important factor during crystallisation, thus demonstrating the delicate balance of intra- and intermolecular forces that is attained during crystallisation. Furthermore, there is an apparent link between the CL-20 molecular conformation adopted in the co-crystal and the polymorph observed after desolvation. In this way, one may conclude that co-crystallisation of energetic materials may provide a highly-selective means of polymorph screening and may, indeed, afford new forms of the unsolvated material.

As has been shown in this study, co-crystallisation often results in a reduction in crystal density and hence one would expect such formulations to exhibit a substantial reduction in explosive power. However, should such energetic co-crystals display sufficiently reduced sensitivity to accidental detonation, it is possible that such formulations may become attractive candidates for insensitive munitions.

**Notes and references**

[‡] Polycrystalline CL-20 was kindly provided by Dstl. **CL-20:DMF** was obtained by rapid crystallisation from a saturated solution of CL-20 (5 mg) in DMF (1 $cm^3$, *ca* 425 K). X-ray single-crystal diffraction data ($\lambda$ = 0.68890 Å) were collected at the Small Molecules Single-Crystal Diffraction Beamline (I19), Diamond Light Source. The crystal was mounted on a diffractometer equipped with a customised Crystal Logic 4-circle $\kappa$ goniometer, a Rigaku Saturn 724 CCD detector and an Oxford Cryostream-*Plus* low-temperature device.[33] Data reduction, including multiscan absorption correction, was performed using the d*TREK software package.[34] The structure was solved[35] and refined by full-matrix least squares against $F^2$, using all data.[36] All non-hydrogen atoms were refined anisotropically; hydrogen atoms were geometrically placed on the parent atoms. X-ray data: $\mu$ = 0.156 $mm^{-1}$, $\theta_{max}$ = 29.4768°, 13 383 reflections measured, 6199 unique ($R_{int}$ = 0.088). Final residuals for 362 parameters were $R_1$ = 0.0645, w$R_2$ = 0.1639 for 6175 data.

**CL-20:dioxane** was obtained by slow crystallisation (several days at 295 K) from a concentrated solution of CL-20 in 1,4-dioxane (10 mg in *ca* 2 $cm^3$). X-ray diffraction intensities were collected using Mo-K$\alpha$ radiation on a Bruker SMART APEX CCD diffractometer equipped with an Oxford Cryostream-Plus low-temperature device.[33] The structure was solved[35] and refined by full-matrix least squares against $F^2$ using all data.[36] One dioxane molecule was best modelled over two positions, each with approximately half-occupancy (0.52, 0.48). All non-hydrogen atoms were refined anisotropically; hydrogen atoms were geometrically placed on the parent atoms. X-ray data: $\mu$ = 0.143 $mm^{-1}$, $\theta_{max}$ = 26.576°, 16 796 reflections measured, 6375 unique ($R_{int}$ = 0.032). Final residuals for 514 parameters were $R_1$ = 0.0738, w$R_2$ = 0.1526 for 6352 data.

**CL-20:HMPA** was obtained by slow crystallisation (1-2 days, 285 – 290 K) from a concentrated solution of 10 mg CL-20 in 2 $cm^3$ hexamethylphosphoramide. X-ray single-crystal diffraction data were collected using Cu-K$\alpha$ radiation on an Oxford Diffraction SuperNova dual wavelength diffractometer equipped with an Atlas CCD detector and an Oxford Cryostream-Plus low-temperature device.[33] Data were integrated and a multi-scan absorption correction was applied using the CrysAlis Pro software package.[37] The structure was solved[35] and refined by full-matrix least squares against $F^2$ using all data.[36] All non-hydrogen atoms were refined anisotropically; hydrogen atoms were geometrically placed on the parent atoms. X-ray data: $\mu$ = 1.953 $mm^{-1}$, $\theta_{max}$ = 73.440°, 43 599 reflections measured, 8920 unique ($R_{int}$ = 0.067). Final residuals for 568 parameters were $R_1$ = 0.0535, w$R_2$ = 0.1370 for 8920 data.

**CL-20:butyrolactone** was obtained by slow crystallisation (several weeks at 295 K) from a concentrated solution of CL-20 in γ-butyrolactone (10 mg in 2$cm^3$). X-ray diffraction intensities were collected using Mo-K$\alpha$ radiation on a Bruker SMART APEX CCD diffractometer equipped with an Oxford Cryostream-Plus low-temperature device.[33] The structure was solved using SUPERFLIP[38] and refined against $F^2$ using full-matrix least squares in CRYSTALS.[36] It was necessary to refine one butyrolactone molecule in two orientations, the occupancies of each were fixed to be 0.5. In order to retain a satisfactorily high data:parameter ratio, it was also necessary to refine all atoms isotropically. Hydrogen atoms were geometrically placed on the parent

atoms. X-ray data: $\mu = 0.173$ mm$^{-1}$, $\theta_{max} = 25.026°$, 6564 reflections measured, all unique ($R_{int} = 0.048$). Final residuals for 582 parameters were $R_1 = 0.0627$, w$R_2 = 0.1337$ for 6542 data.


[1] Section B8 (General Munitions and Energetic Technologies), *Defence Technology Strategy,* UK Ministry of Defence, October 2006.

[2] R.M. Doherty and D.S. Watt, *Propellants, Explos., Pyrotech.*, 2008, **33**, 4-13.

[3] U. Bemm and H. Ostmark, *Acta Cryst.*, 1998, **C54**, 1997-1999.

[4] K.B. Landenberger and A.J. Matzger, *Cryst. Growth Des.*, 2010, **10**, 5341-5347.

[5] D.I.A. Millar, L.K. Cocker, D.R. Allan, A.S. Cumming, C.A. Morrison and C.R. Pulham, *submitted to CrystEngComm*, 2011.

[6] N. Blagden, D.J. Berry, A. Parkin, H. Javed, A. Ibrahim, P.T. Gavan, L.L. De Matos and C.C. Seaton, *New J. Chem.*, 2008, **32**, 1659-1672.

[7] C.B. Aakeroy, J. Desper, M. Fasulo, I. Hussain, B. Levin and N. Schultheiss, *CrystEngComm*, 2008, **10**, 1816-1821.

[8] S.L. Childs and M.J. Zaworotko, *Cryst. Growth Des.*, 2009, **9**, 4208-4211.

[9] O. Almarsson and M.J. Zaworotko, *Chem. Commun.*, 2004, 1889-1896.

[10] N. Rodriguez-Hornedo, *Mol. Pharmaceutics*, 2007, **4**, 299-300.

[11] W. Selig, *Propellants, Explos., Pyrotech.*, 1981, **6**, 1-4.

[12] W. Selig, *Propellants, Explos., Pyrotech.*, 1982, **7**, 70-77.

[13] R.S. George, H.H. Cady, R.N. Rogers and R.K. Rohwer, *Ind. Eng. Chem. Prod. Res. Dev.*, 1965, **4**, 209-214.

[14] R.E. Cobbledick and R.W.H. Small, *Acta Cryst.*, 1975, **B31**, 2805-2808.

[15] T.M. Haller, A.L. Rheingold and T.B. Brill, *Acta Cryst.*, 1985, **C41**, 963-965.

[16] T.M. Haller, T.B. Brill and A.L. Rheingold, *Acta Cryst.*, 1984, **C40**, 517-519.

[17] A.T. Nielsen, A.P. Chafin, S.L. Christian, D.W. Moore, M.P. Nadler, R.A. Nissan, D.J. Vanderah, R.D. Gilardi, C.F. George and J.L. Flippen-Anderson, *Tetrahedron*, 1998, **54**, 11793-11812.

[18] R.L. Simpson, P.A. Urtiew, D.L. Ornellas, G.L. Moody, K.J. Scribner and D.M. Hoffman, *Propellants, Explos., Pyrotech.*, 1997, **22**, 249-255.

[19] D. Mueller, *Propellants, Explos., Pyrotech.*, 1999, **24**, 176-181.

[20] U.R. Nair, R. Sivabalan, G.M. Gore, M. Geetha, S.N. Asthana and H. Singh, *Combustion, Explosion, and Shock Waves*, 2005, **41**, 121-132.

[21] S.S. Samudre, U.R. Nair, G.M. Gore, R.K. Sinha, A.K. Sikder and S.N. Asthana, *Propellants, Explos., Pyrotech.*, 2009, **34**, 145-150.

[22] T.P. Russell, P.J. Miller, G.J. Piermarini and S. Block, *J. Phys. Chem.*, 1993, **97**, 1993-1997.

[23] D.I.A. Millar, H.E. Maynard-Casely, A.K. Kleppe, W.G. Marshall, C.R. Pulham and A.S. Cumming, *CrystEngComm*, 2010, **12**, 2524-2527.

[24] Y. Kholod, S. Okovytyy, G. Kuramshina, M. Qasim, L. Gorb and J. Leszczynski, *J. Mol. Struct.*, 2007, **843**, 14-25.

[25] Y.X. Ou, H.P. Jia, B.R. Chen, Y.J. Xu, J.T. Chen and R.X. Xu, *Youji Huaxue*, 1999, **19**, 500-507.

[26] N.B. Bolotina, M.J. Hardie, R.L. Speer Jr and A.A. Pinkerton, *J. Appl. Crystallogr.*, 2004, **37**, 808-814.

[27] M.F. Foltz, C.L. Coon, F. Garcia and A.L. Nichols III, *Propellants, Explos., Pyrotech.*, 1994, **19**, 19-25.

[28] V. Favre-Nicolin and R. Cerny, *J. Appl. Crystallogr.*, 2002, **35**, 734-743.

[29] X. Zhao and J. Liu, *Beijing Ligong Daxue Xuebao*, 1996, **16**, 494-497.

[30] S. Jin, S. Chen and X. Lei, *Binggong Xuebao*, 2008, **29**, 90-93.

[31] S. Saint Martin, S. Marre, P. Guionneau, F. Cansell, J. Renouard, V. Marchetto and C. Aymonier, *Chem. Eur. J.*, 2010, **16**, 13473-13478.

[32] J. Akhavan, *The Chemistry of Explosives*, Royal Society of Chemistry, Cambridge, UK, 2004.

[33] J. Cosier and A.M. Glazer, *J. Appl. Crystallogr.*, 1986, **19**, 105-107.

[34] J. Pflugrath, *Acta Cryst.*, 1999, **D55**, 1718-1725.

[35] A. Altomare, G. Cascarano, C. Giacovazzo, A. Guagliardi, M.C. Burla, G. Polidori and M. Camalli, *J. Appl. Crystallogr.*, 1994, **27**, 435.

[36] P.W. Betteridge, J.R. Carruthers, R.I. Cooper, K. Prout and D.J. Watkin, *J. Appl. Crystallogr.*, 2003, **36**, 1487.

[37] *CrysalisPRO*, Oxford Diffraction Ltd, Abingdon, UK, 2010.

[38] L. Palatinus and G. Chapuis, *J. Appl. Crystallogr.*, 2007, **40**, 786-790.